

Dynamical effects in diffuse neutron scattering by low-dislocation-density germanium

Yu. G. Abov, A. O. Eidlin, D. S. Denisov, N. O. Elyutin, and S. K. Matveev

Moscow Engineering Physics Institute, 115409 Moscow, Russia

(Submitted 19 May 1993)

Zh. Eksp. Teor. Fiz. **104**, 4072–4080 (December 1993)

We have developed a method for separating diffuse and dynamical components of neutron radiation diffracted by a thick crystal with structural defects. The method is based on spatial scanning of a narrow monochromatic Bragg-reflected beam. Dynamical effects have been observed in diffuse scattering, in particular, interference bands, similar to Pendellösung beats in the diffraction by perfect crystals.

The behavior observed in diffuse scattering accompanying diffraction by real crystals is, as a rule, well described by the kinematic theory of diffraction,¹ in which effects due to multiple scattering and complicated interference interaction of waves are negligible. However, for sufficiently perfect crystals, which are widely employed due to the development of semiconductor technology, the regions of coherent scattering are significantly larger. For this reason, dynamical diffraction of incident and diffusely scattered waves plays a significant role in the case of large defects, which scatter radiation by small angles, and this results in interference Pendellösung beats, anomalous transmission of diffuse intensity, significant distortion of isodiffuse lines, and so on.^{2–8}

In the experimental study of diffuse scattering the diffuse component must be separated from the strong dynamical background peak. The methods used for measuring the integral intensity of diffracted radiation,^{9–11} as a rule, involve fitting the experimental data with some theoretical model, and this presupposes the existence of *a priori* information about the nature of the defects of the crystal structure. Due to the relatively low intensity of diffuse scattering the results of such analysis are often of doubtful reliability, something which is, however, inherent to most indirect methods of measurement. The three-crystal spectrometer method, which makes it possible to resolve the diffuse peak from the dynamical components of the reflected beam, does not have these deficiencies.¹² The x-ray variant of this technique has been used in a number of works,^{13–15} confirming the results of theoretical calculations.^{2–8}

In the present work, in order to separate the diffuse and dynamical components of the reflected beam we employed the fact that in the case of a thick perfect crystal and Bragg geometry the bulk of the crystal does not “participate” in neutron reflection. The method is based on spatial scanning of the diffracted radiation¹⁶ with a narrow monochromatic neutron beam incident on the sample. The layout of the experiment, performed using setup of Ref. 17, is displayed in Fig. 1. A monochromatic neutron beam, formed by (1,1,1) reflection of reactor radiation from a germanium monochromator with the half-width of the reflection curve equal to 6 angular minutes was limited by the diaphragm *S1* with a $0.3 \times 10 \text{ mm}^2$ rectangular window and directed on the experimental Ge sample, positioned at

the Bragg angle θ_B . The spatial distribution of the diffracted radiation was scanned by stepping an identical diaphragm *S2* in a direction perpendicular to the reflected beam in the diffraction plane, after which the beam was recorded with the help of a stationary detector. The neutron wavelength was $\lambda = 1.84 \text{ \AA}$ and the nonmonochromaticity $\Delta\lambda/\lambda = 0.01$; all experimental samples were subjected to standard procedures of chemical-mechanical and chemical polishings in order to remove the damaged layer. Due to extinction of the incident radiation within the angular interval of the Bragg peak (under these conditions the width of the plateau of the “Darwin table” is 2.1 angular seconds and the extinction length is $\Delta_0 = 18.6 \text{ \mu m}$) the scanned distribution contains an intense peak corresponding to reflection from the surface layer of the sample (see Fig. 1 and Fig. 2a). The part of the beam passing into the crystal is reflected from the back surface of the crystal, and this gives rise to a second asymmetric peak with a continuously decaying “right-hand tail.” This is due to a well-known effect which accompanies Bragg reflection and is similar to the Bormann fan in Laue diffraction.¹⁸ Thus for a perfect crystal with a “frozen” lattice the intensity of the diffracted radiation should be zero in the region between the dynamical peaks. This is demonstrated by the fact that the distribution measured for a 3.68 mm thick dislocation-free Ge crystal (dislocation density less than 10 cm^{-2}) is identical to the curve calculated for the experimental conditions with the help of the dynamical theory.¹⁹ Measurements on a two-crystal spectrometer, employing crystals of this type and the (1,1,1) reflection, showed that to within the experimental error, the half-width of the rocking curve $\omega = 2.9 \pm 0.2$ angular seconds agrees with the computed value. In addition, investigations on a three-crystal spectrometer²⁰ have demonstrated that there is no diffuse scattering for this sample. In the case of a sufficiently perfect crystal with defects the recorded distribution should not change radically. Due to the existence of lattice distortions, however, the “transilluminated volume” of the sample becomes a source of diffuse waves, and as a result diffuse scattering is recorded in the region between the dynamical peaks. This is confirmed by investigations performed using both neutron and x-ray beams.^{21–22} We emphasize that in the present experiment the recorded intensity of the diffuse scattering is an angle-integrated quantity because of the relatively large aperture of the diaphragms

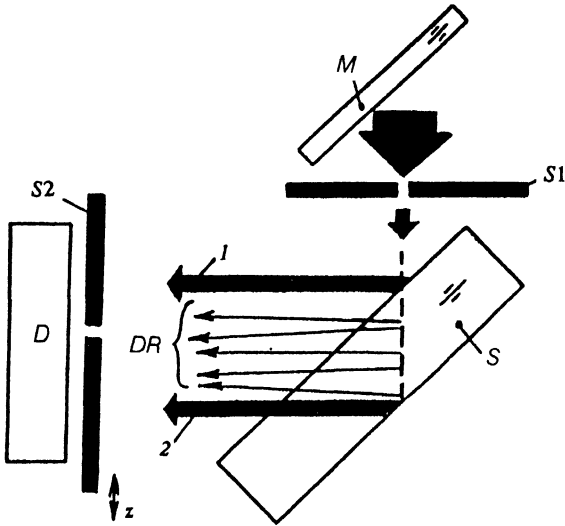


FIG. 1. Layout of experiment on scanning the spatial distribution of a beam reflected by the sample: *S1* and *S2*—limiting and scanning diaphragms, respectively; *S*—sample; *D*—detector; the arrows 1 and 2 indicate the dynamical components of the diffracted radiation (rays reflected from the surface layer due to extinction and the beam reflected from the back surface of the crystal, respectively); *DR*—diffuse radiation, scattered by the volume of the sample; the arrow *z* indicates the direction of motion of the diaphragm *S2*.

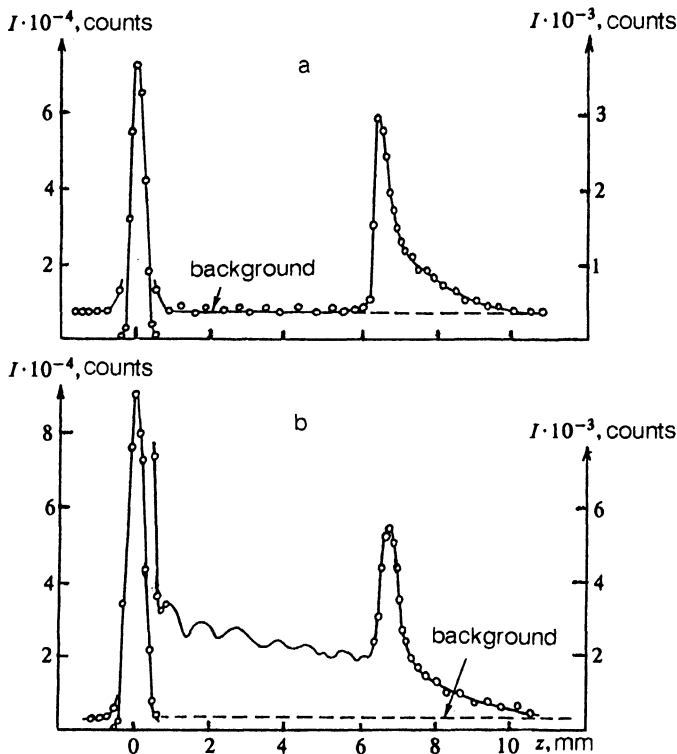


FIG. 2. Measured spatial distributions of the diffracted radiation (the extinction peak is shown on a smaller scale): a) Distribution obtained for dislocation-free germanium; here the solid line designates the curve calculated from the dynamical theory for the experimental conditions; b) The curve for the sample with dislocation density $\sim 900 \text{ cm}^{-2}$.

S1 and *S2*. Figure 2b displays the results obtained for a 3.55 mm thick sample with dislocation density $\sim 900 \text{ cm}^{-2}$. For this crystal the half-width of the rocking curve of the two-crystal spectrometer is somewhat larger than the computed value and is equal to $\omega = 3.6 \pm 0.3$ angular seconds. Measurements in the three-crystal method showed the presence of a fairly intense diffuse peak in the angular distributions.²⁰ As is evident from Fig. 2b, a non-uniform distribution of diffuse scattering is observed between the dynamical peaks. The overall dropoff in the intensity of diffuse scattering as a function of the position *z* of the scanning diaphragm is partially associated with normal absorption and incoherent and thermal diffuse neutron scattering in the sample.

Beats in the intensity of diffuse scattering are of a special interest. They are displayed in an enlarged scale in Fig. 3a. Similar interference bands have been observed by the method of x-ray topography on curved perfect crystals,²³ and their origin was explained in Ref. 24. According to the latter work, in the case of a deformed perfect crystal the trajectories of the Bloch waves acquire a hyperbolic form for one of the dispersion surfaces¹⁸ (the particular surface depends on the sign of the deformation). The Bloch waves reflecting periodically at some depth, which is determined by the position of the point of excitation on the dispersion surface (glancing angle), return to the entrance surface of the crystal, where partial reflection can likewise occur. Interference of waves arriving at the same point of the surface with a different number of internal reflections gives rise to beats of the intensity at the exit from the sample. In the case of uniform deformation the coordinates x_n of the maxima, measured from the point of incidence of the beam on the crystal along the surface of the crystal plate, satisfy the following relation:²⁴

$$x'_n = [16\pi(2n-1)/5B'^2]^{1/3}. \quad (1)$$

Here n is the number of the maximum (see Fig. 3a); $x' = \pi x / \Delta_0$; $B' = B \Delta_0^2 / \pi^2$; $B = \frac{1}{4} d^2 (\vec{h} \vec{u}) / \partial S_0 \partial S_h$ is the gradient of the deformation, \vec{h} and \vec{u} are, respectively, a reciprocal lattice vector and the deformation vector; and, \vec{S}_0 and \vec{S}_h are the unit vectors of the standard oblique coordinate system employed for describing diffraction. If the uniform diffraction is caused by the curvature of the crystal plate, then the radius of curvature is

$$R = \Delta_0^2 / 2\pi d t g^2 \theta_B B', \quad (2)$$

where d is the interplanar separation. This is what made it possible in Ref. 23 to determine from the deformation interference bands the value of R for a silicon plate with an amorphous oxide film grown on its surface.

Figure 3b displays a graph of $x'_n(n)$, calculated from the data presented in Fig. 3a. As one can see, contrary to Eq. (1), points with $n=1$ and $n=2$, in general, do not lie on a straight line. The value of the reduced deformation gradient was determined from the linear section using the formula (1): $B' = (5.0 \pm 0.1) \cdot 10^{-5}$. Next, the equation (2) was used to calculate $R = 39 \pm 1 \text{ km}$ under the assumption that the observed oscillations are caused by the curvature of the crystal. Additional measurements were per-

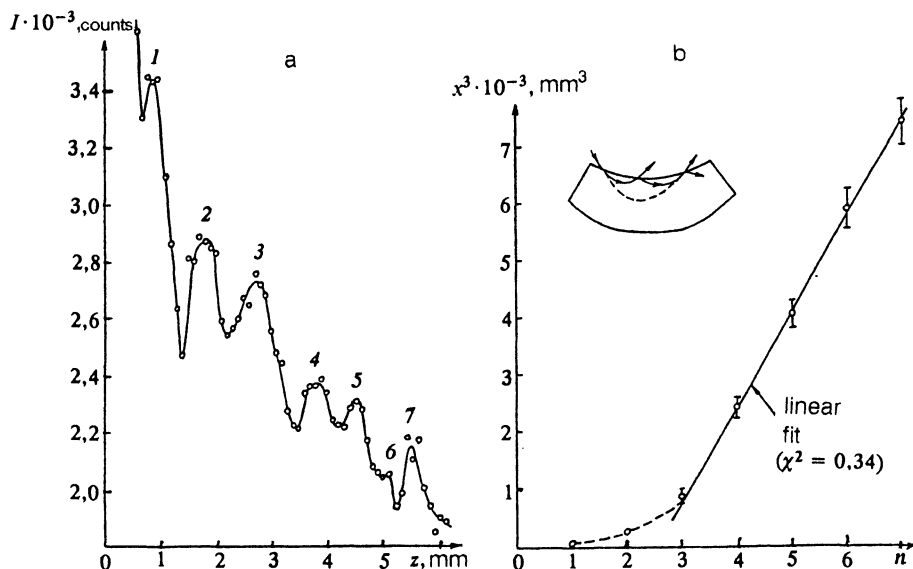


FIG. 3. Interference bands observed in diffraction by a sample with dislocations: a) Portion of the spatial distribution between the dynamical peaks. The fragment is shown on a larger scale than in Fig. 2b; here 1, 2, ..., 7 are the numbers of the maxima of the observed beats; b) plot of $x_n^3(n)$, where n is the number of the maximum and x_n is the location of the maximum, measured from the location of incidence of the primary beam on the surface of the crystal plate. Inset: Trajectories of Bloch waves in the case of diffraction by a curved perfect crystal.

formed in the two-crystal parallel spectrometer method²⁵ in order to determine the radius of curvature of the experimental crystal. In these measurements characteristic features of the neutron diffraction method were employed, such as a wide (\sim several cm) beam and large detector dimensions. The first crystal consisted of a perfect single crystal of germanium and the second crystal was the sample placed in the path of the beam. A $0.3 \times 10 \text{ mm}^2$ diaphragm was placed between the crystals on the alignment table. The "illuminated spot" is moved along the surface of the experimental crystal by changing the position of the diaphragm. In the case of a curved sample the rocking curves²⁵ measured for different positions of the diaphragm exhibit an angular shift a , from whose sign and magnitude the sign and radius of curvature of the single-crystalline plate are determined easily. Here $R = l/a$, where l is the linear displacement of a neutron "beam" along the surface of the crystal. For an experimental sample with $l = 70 \text{ mm}$ we find $a = 0$ within the experimental error ($\sim 0.3''$). This gave a lower limit of the radius of curvature of at least 50 km.

This makes it possible to conclude that the observed beats are not associated, at least, with the curvature of the crystal. Nonetheless, it can be conjectured that the observed oscillations are caused by the random, possibly, nonuniform deformation which arises in the crystal, for example, when the crystal is worked. This, by the way, would explain why the plot of $x_n^3(n)$ is not a straight line.

In order to check this proposition we performed the experiment whose layout is displayed in Fig. 4a. In this experiment the dimensions of the diaphragm $S1$ were $0.3 \times 10 \text{ mm}^2$, and the window of the diaphragm $S2$ was increased to $1.8 \times 10 \text{ mm}^2$ because of the low counting rate at the detector. The position of $S2$ was chosen so that only rays emanating from the interior of the sample reached the analyzer crystal. The angular distribution of the radiation propagating from the volume of the crystal was scanned by rotating the analyzer in steps and by exposing the beam reflected from it. Figure 4b displays the results of these

measurements, obtained for different positions of the diaphragm $S2$. As one can see, for the same overall form of the angular distributions the intensity decreases as a function of the coordinate z of the diaphragm $S2$. This is associated with the absorption and incoherent and thermal diffuse scattering of neutrons in the sample. The angular coordinate of the minimum of the observed dip is identical to the position of the maximum of the extinction peak, corresponding to rays reflected from the surface layer of the sample. Thus the double-hump form of the measured distributions is due to the "eating away" of the primary peak by extinction. The obtained curves indicate the existence of deformations with alternating signs in the volume of the sample. Indeed, when the sign of the gradient of the deformation remains constant, Bloch waves for only one of the dispersion branches undergo internal reflection in the volume of the crystal. Thus, in this case, the angular distributions must be sharply asymmetric with respect to the Bragg angle. Moreover, the observed spatial and angular distributions did not change as the "illuminated spot" moved along the surface of the sample, and also when the beam was directed on the back surface of the crystal. Investigations of several plates, fabricated from the same Ge single crystal (with dislocation density $\sim 900 \text{ cm}^{-2}$), showed that oscillations in the spatial distributions are observed for all of them. All this leads to the conclusion that the present methods recorded diffuse scattering, caused by bulk distortions of the lattice of alternating sign, from defects of the crystal structure, and the oscillations in the spatial distributions are analogous to Pendellösung beats in the diffraction by a perfect crystal. The somewhat higher intensity in the distributions obtained at smaller glancing angles and displayed in Fig. 4b can be explained by the well-known interference character of absorption near the Bragg angle,²⁵ as manifested in the asymmetric form of the reflection curve (Prince's curve) in the case of Bragg diffraction by an ideal crystal. The rocking curves of the two-crystal spectrometer, in which one of the crystals was the sample with dislocations, are also asymmetric. This is a

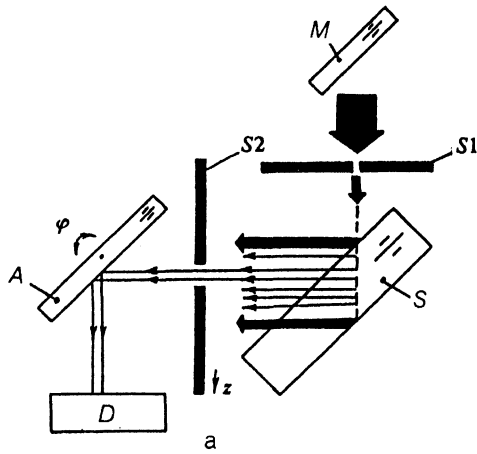
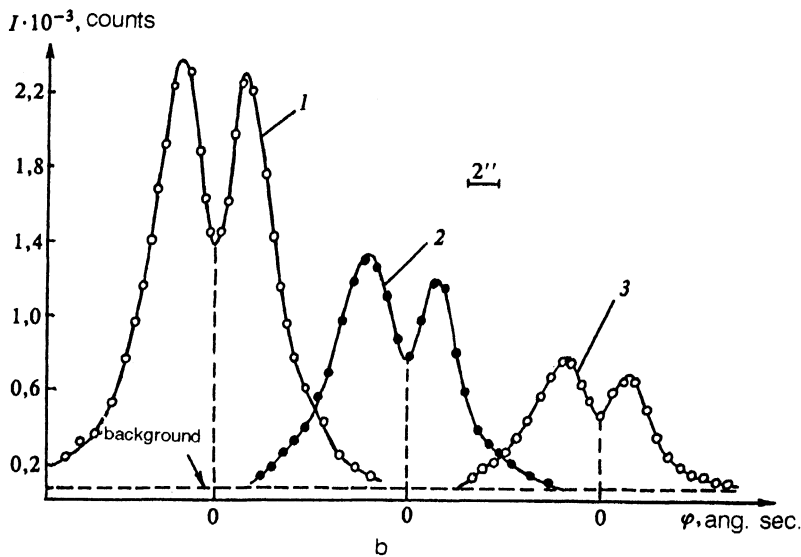


FIG. 4. Measurement of the angular distributions of the diffuse component of the beam reflected by a crystal with dislocations: a) Layout of experiment: *M*—monochromator; *S1* and *S2*—limiting and scanning diaphragms, respectively (the arrow *z* indicates the direction of motion of *S2*); *S*—sample; *A*—analyzer crystal (the arrow φ indicates the direction of rotation of the analyzer during scanning of the angular distribution); *D*—detector; b) resulting angular distributions of diffuse intensity; the curves 2 and 3 were measured with the diaphragm *S2* displaced in the direction indicated in Fig. 4a by 0.7 and 1.4 mm, respectively, with respect to the position of *S2* in the case of scanning of curve 1.



manifestation of the effect observed in Fig. 4b.

Returning to the spatial distributions displayed in Figs. 2b and 3a, it should be noted that the value of the linear attenuation coefficient $\mu^{\text{exp}} = 0.28 \text{ cm}^{-1}$, determined from the total dropoff in the diffuse reflection intensity averaged over the oscillations, is almost twice the corresponding value $\mu' = 0.15 \text{ cm}^{-1}$ calculated taking into account absorption as well as incoherent and thermal diffuse scattering. The linear attenuation coefficient, associated with thermal diffuse scattering and equal to $\mu^{\text{tds}} = 3.6 \cdot 10^{-2} \text{ cm}^{-1}$, was calculated by the method of Refs. 26–27. The experimental value of the linear attenuation coefficient is larger than the calculated value because of extinction of the transmitted wave due to diffuse scattering; this fact was previously observed in Ref. 22 with x-ray radiation. Thus the angle-integrated attenuation coefficient, determined by diffuse scattering, for the transmitted wave can be calculated from the experimental data: $\mu^{\text{ds}} = 0.13 \text{ cm}^{-1}$. In Ref. 3 approximate formulas expressing μ^{ds} in terms of the concentration and characteristic size of the nonuniformities were derived for several types of defects. For this reason, when *a priori* information about the nature of defects of the crystal structure is available, the characteristic size and concentration of nonuniformities can be determined simultaneously by performing direct measurements of μ^{ds} , by the

method described above, for different reflections or wavelengths.

In conclusion, it should be noted that the dynamical and diffuse components of radiation diffracted by a slightly distorted crystal can be measured separately with the help of relatively simple methods. A number of theoretically predicted dynamical effects in diffuse scattering were observed and qualitatively explained: suppression of diffuse scattering in the Bragg direction, interference character of the absorption of the diffuse scattering near the Bragg angle, and a pronounced coherent effect—Pendellösung bands, observed for the first time in diffuse scattering. It would be of great interest to compare the results described above to data obtained by the same method with the help of x-ray radiation. Unfortunately, however, measurements of x-ray Bragg section topograms for the experimental samples were unsuccessful because of the strong absorption of x-rays in germanium. The present work is, to all appearances, not just a demonstration of interesting coherent effects in, generally speaking, incoherent phenomena such as diffuse neutron scattering. By analyzing this question theoretically the observed Pendellösung beats could yield information about defects of the crystal lattice in relatively perfect crystals, and the method described could become

an effective supplement to traditional topographic and three-crystal methods.

We thank F. N. Chukhovskii for helpful discussions and V. I. Polovinkin for performing the x-ray measurements.

Financial support of this work was provided by the Russian Foundation for Fundamental Research (No. 93-0-14680).

- ¹M. A. Krivoglaz, *Diffraction of X-Rays and Neutrons in Imperfect Crystals* [in Russian], Naukova dumka, Kiev, 1983.
- ²V. V. Molodkin, *Metallofiz.* **2**, 3 (1980).
- ³V. B. Molodkin, *Metallofiz.* **3**, 27 (1981).
- ⁴V. B. Molodkin, S. I. Olikhovskii, and M. E. Osinovskii, *Metallofiz.* **5**, 3 (1983).
- ⁵V. M. Kaganer and V. L. Indenbom, *Metallofiz.* **8**, 25 (1986).
- ⁶A. M. Afanas'ev and V. G. Kohn, *Acta Crystallogr. A* **27**, 421 (1971).
- ⁷A. M. Polyakov, F. N. Chukhovskii, and D. I. Piskunov, *Zh. Eksp. Teor. Fiz.* **99**, 589 (1991) [*Sov. Phys. JETP* **72**, 330 (1991)].
- ⁸S. L. Dudarev, *Kristallografiya* **35**, 1332 (1990) [*Sov. Phys. Crystallogr.* **35**, 785 (1990)].
- ⁹J. R. Patel, *J. Appl. Cryst.* **8**, 186 (1975).
- ¹⁰S. N. Voronkov, D. I. Piskunov, F. N. Chukhovskii, and S. K. Maksimov, *Zh. Eksp. Teor. Fiz.* **92**, 1009 (1987) [*Sov. Phys. JETP* **65**, 624 (1987)].
- ¹¹V. B. Molodkin, L. I. Datsenko, V. I. Khrupa, M. E. Osinovskii, E. N. Kislovskii, V. P. Klad'ko, and N. V. Osadchaya, *Metallofiz.* **5**, 7 (1983).
- ¹²B. C. Larson and W. Schmatz, *Phys. Rev. B* **10**, 2307 (1974).
- ¹³V. V. Ratnikov and L. M. Sorokin, *Fiz. Tverd. Tela* **26**, 2445 (1984) [*Sov. Phys. Solid State* **26**, 2070 (1984)].
- ¹⁴R. N. Kyutt and V. V. Ratnikov, *Metallofiz.* **7**, 36 (1985).
- ¹⁵V. V. Ratnikov, E. K. Kov'ev, and L. M. Sorokin, *Fiz. Tverd. Tela* **26**, 2155 (1984) [*Sov. Phys. Solid State* **26**, 1305 (1984)].
- ¹⁶A. O. Eidlin, S. K. Matveev, N. O. Elyutin, and F. G. Kulidzhanov, *Inventor's Certificate No. 1312460. Otkrytiya. Izobreteniya*, No. 19, 75 (1987).
- ¹⁷Yu. G. Abov, F. G. Kulidzhanov, N. O. Elyutin, and S. N. Nizovoi, *Prib. Tekh. Eksp.*, No. 4, 52 (1984).
- ¹⁸H. Rauch and D. Petrascheck, *Dynamical Neutron Diffraction. Topics in Current Physics*, Springer Verlag, New York, 1979, pp. 303–351.
- ¹⁹A. O. Eidlin, S. K. Matveev, and N. O. Elyutin, Preprint No. 22-88, Moscow Engineering Physics Institute, Moscow, 1988.
- ²⁰F. G. Kulidzhanov, A. O. Eidlin, and N. O. Elyutin, *Pis'ma Zh. Tekh. Fiz.* **12**, 1003 (1986) [*Sov. Tech. Phys. Lett.* **12**, 414 (1986)].
- ²¹A. Zeilinger, C. G. Shull, J. Arthur, and M. A. Horn, *Phys. Rev. A* **28**, 487 (1983).
- ²²V. I. Zhurpa and I. R. Entin, *Metallofiz.* **13**, 117 (1991).
- ²³P. V. Petrashen', F. N. Chukhovskii, I. L. Shul'pina, and R. N. Kyutt, *Fiz. Tverd. Tela* **29**, 1608 (1987) [*Sov. Phys. Solid State* **29**, 927 (1987)].
- ²⁴F. N. Chukhovskii and P. V. Petrashen, *Acta Crystallogr. A* **44**, 8 (1988).
- ²⁵Z. G. Pinsker, *X-Ray Crystal Optics* [in Russian], Nauka, Moscow, 1982.
- ²⁶A. Z. Men'shikov, S. G. Bogdanov, Yu. M. Plishkin, V. V. Dyakin, and N. N. Lebedeva in *Neutron Diffraction Analysis of Metals, Alloys, and Compounds* [in Russian], Institute of Metal Physics, Ural Scientific Center, Academy of Sciences of the USSR, Sverdlovsk, 1977, pp. 89–107.
- ²⁷L. I. Mirkin, *Handbook of X-Ray-Structural Analysis of Polycrystals* [in Russian], Fizmatgiz, Moscow, 1961.

Translated by M. E. Alferieff